Critical Fragmentation Properties of Random Drilling: How Many Holes Need to Be Drilled to Collapse a Wooden Cube?

K. J. Schrenk,[1,2,*] M. R. Hilário,[3,4,†] V. Sidoravicius,[5,6,7,‡] N. A. M. Araújo,[8,§] H. J. Herrmann,[1,9,‖] M. Thielmann,[10,¶] and A. Teixeira[11,**]

[1]*Computational Physics for Engineering Materials, IfB, ETH Zurich, Wolfgang-Pauli-Strasse 27, CH-8093 Zurich, Switzerland*
[2]*Department of Chemistry, University of Cambridge, Lensfield Road, Cambridge CB2 1EW, United Kingdom*
[3]*Departamento de Matemática, Universidade Federal de Minas Gerais, Avenida Antonio Carlos, 6627—P.O. Box 702–30161-970, Belo Horizonte, Minas Gerais, Brazil*
[4]*Section de Mathématiques, Université de Genève, 2-4 Rue du Lièvre, 1211 Genève, Switzerland*
[5]*Courant Institute of Mathematical Sciences, New York University, 251 Mercer Street, New York, New York 10012, USA*
[6]*New York University—Shanghai, 1555 Century Avenue, Pudong New Area, Shanghai 200122, China*
[7]*CEMADEN, Avenida Doutor Altino Bondensan, 500, São José dos Campos, São Paulo 12247-016, Brazil*
[8]*Departamento de Física, Faculdade de Ciências, Universidade de Lisboa, 1749-016 Lisboa, Portugal and Centro de Física Teórica e Computacional, Universidade de Lisboa, 1749-016 Lisboa, Portugal*
[9]*Departamento de Física, Universidade Federal do Ceará, 60451-970 Fortaleza, Ceará, Brazil*
[10]*Bayerisches Geoinstitut, University of Bayreuth, Universitätsstraße 30, 95440 Bayreuth, Germany*
[11]*Instituto Nacional de Matemática Pura e Aplicada, Est. Dona Castorina, 110, 22460-320 Rio de Janeiro, Rio de Janeiro, Brazil*

(Received 9 November 2015; published 2 February 2016)

A solid wooden cube fragments into pieces as we sequentially drill holes through it randomly. This seemingly straightforward observation encompasses deep and nontrivial geometrical and probabilistic behavior that is discussed here. Combining numerical simulations and rigorous results, we find off-critical scale-free behavior and a continuous transition at a critical density of holes that significantly differs from classical percolation.

DOI: 10.1103/PhysRevLett.116.055701

The connectivity of a solid block of material strongly depends on the density of defects. To systematically study this dependence, one must find an experimental way to create defects inside the solid. For example, in 2D, one can simply punch holes in a sheet and measure the physical properties of the remaining material. But in 3D, inducing localized defects is not simple. One conventional solution consists in perforating the material by drilling holes or laser ablation from the surface [1,2].

In a tabletop experiment, we start with a solid cube of wood and plot on each face a square-lattice mesh of L by L cells. Initially, the cube has no holes. Sequentially, for each one of three perpendicular faces, we randomly choose one square cell and drill a hole having a radius of $1/\sqrt{2}$ cell lengths to the other side of the cube. We repeat this process iteratively until the entire structure collapses into small pieces and the bottom and top part of the cube are no longer connected. The first row of Figs. 1(a)–1(d) shows the result of the drilling process of a real cube with edge length 6 cm (manufactured from 2 cm thick plates of medium-density fiberboard), where holes were drilled with a diameter of 1 cm. As the drilling proceeds, pieces get disconnected and eventually the entire structure collapses.

Numerically, we start with a three-dimensional cubic lattice of L^3 sites and fix three perpendicular faces. A fraction $1-p$ square cells on each face is randomly selected, and all sites along the line perpendicular to that face are removed (second row of Fig. 1). Thirty years ago, Y. Kantor [3] numerically studied this model on lattices of up to 10^6 sites and concluded that the critical fragmentation properties of this model are in the same universality class as random percolation [4–6]. Here, we combine rigorous results and large-scale numerical simulations, considering lattices 3 orders of magnitude larger in size, to show that

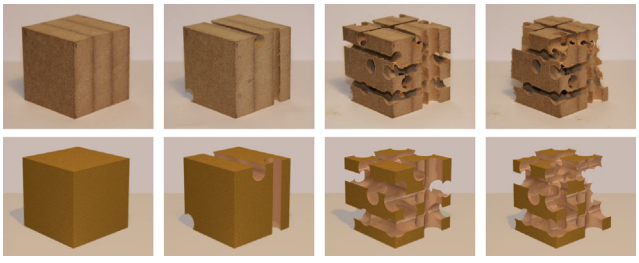

FIG. 1. Cube drilling. The upper row shows photos of the experimental setup; the lower panels are the corresponding numerical results. The faces of the cube are divided with a square-lattice mesh of linear size $L = 6$, such that each face can be drilled $L^2 = 36$ times. From left to right, (a)–(d), the number of drilled holes per face are (a) 0, (b) 1, (c) 6, and (d) 8. From our numerical results for the position of the transition in the thermodynamic limit (see main text), one estimates that around 13 holes need to be drilled for the cube to disconnect.

this is not the case. Removing entire rows at once induces strong long-range directional correlations, and the critical behavior departs from random percolation. Also remarkably, while in random fragmentation power-law scaling is solely observed around the critical threshold, here we find it in an entire off-critical region. These findings suggest that long-range directional correlations lead to a rich spectrum of critical phenomena which need to be understood. Possible implications for other complex percolation models are discussed in the conclusions.

Threshold.—The average total number of drilled holes is $3(1-p)L^2$, and the asymptotic probability that a site in the bulk is not removed is p^3. We first measure the threshold p_c at which the cube collapses for different lattice sizes, up to $L = 1024$, using different estimators of the transition point, as discussed in the Supplemental Material [7]. Extrapolating the data to the limit $L \to \infty$ gives $p_c = 0.6339 \pm 0.0005$, consistent with the value estimated by Kantor using Monte Carlo renormalization group techniques [3] (see Supplemental Material [7]). This threshold is larger than the two-dimensional square-lattice percolation threshold (p_{2D}) [35,36] and smaller than the cubic root of the one for the three-dimensional simple cubic lattice [37].

Static exponents.—We consider the fraction P_∞ of sites in the largest cluster of connected sites [see Supplemental Material for more data of $P_\infty(p)$ and of other observables [7]]. P_∞ is the standard order parameter in percolation identifying the transition from a disconnected to a globally connected state. For the drilling model, the situation will turn out to be more complicated. Figure 2(a) shows a double-logarithmic plot of the order parameter, rescaled by a power of the lattice size $P_\infty L^{\beta/\nu}$ as a function of the distance to the transition $|p-p_c|L^{1/\nu}$. Based on finite-size scaling analysis [5], we find that the critical exponent of the order parameter is $\beta = 0.52 \pm 0.04$, and the inverse of the correlation length exponent is $1/\nu = 0.92 \pm 0.01$ (see Supplemental Material [7]). We note that both β and ν are different from the corresponding values for 2D and 3D classical percolation. However, somehow surprisingly, the exponent ratio $\beta/\nu = 0.50 \pm 0.04$ is within error bars the same as for 3D percolation. Thus, while the fractal dimension of the largest cluster (given by $d_f = d - \beta/\nu$) is consistent with the one for 3D percolation, the larger value of β (compared to 3D percolation) implies that the transition from the connected to the disconnected state is less abrupt (see also Supplemental Material [7]). We consider next the behavior of the second moment of the cluster size distribution M_2', excluding the contribution of the largest cluster. As shown in Fig. 2(b), the finite-size scaling analysis gives that the susceptibility critical exponent is $\gamma = 2.3 \pm 0.1$. We note that our results for the static critical exponents are within error bars consistent with the scaling relation $2\beta + \gamma = d\nu$ (for $d = 3$).

Dynamical exponents.—The transport properties of the largest cluster at the critical threshold, p_c, are intimately related to dynamical critical exponents, and they can be measured by quantifying three sets of sites in the largest

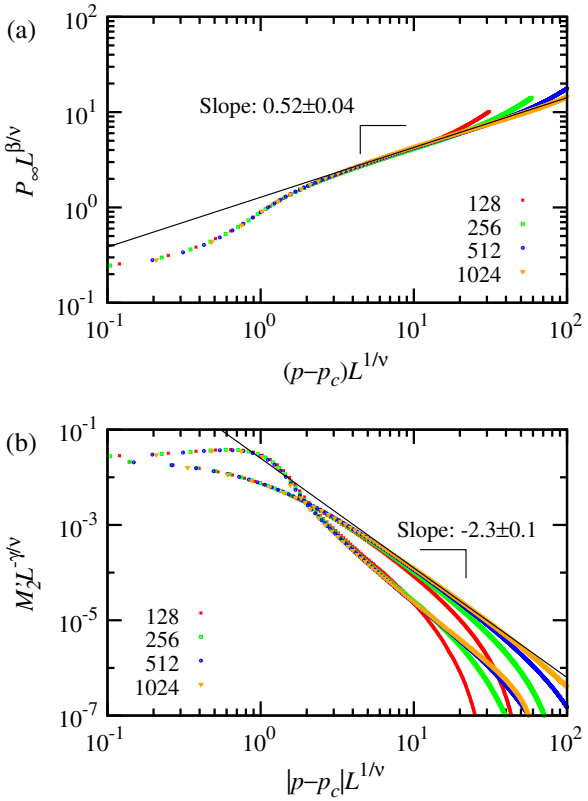

FIG. 2. (a) Double-logarithmic plot of the rescaled order parameter $P_\infty L^{\beta/\nu}$ as a function of the scaling variable $(p-p_c)L^{1/\nu}$ for different lattice sizes L. The linear part has a slope of $\beta = 0.52 \pm 0.04$, consistent with β/ν being the same as for three-dimensional percolation, but with a different exponent $1/\nu = 0.92$. The present value of β is different from the two-dimensional one $\beta = 5/36 \approx 0.139$ [5,38] and the one in three dimensions, $\beta \approx 0.417$ [39]. (b) Double-logarithmic plot of the rescaled second moment $M_2' L^{-\gamma/\nu}$, with $\gamma/\nu = 2.0452$, as a function of the scaling variable $|p-p_c|L^{1/\nu}$, with $1/\nu = 0.92$, for different lattice sizes L. The solid black line is a guide to the eye with a slope -2.3. The two sets of data correspond to the subcritical ($p < p_c$) and supercritical ($p > p_c$) regions.

cluster [40]. First, we consider the so-called red sites. A site is considered a red site if its removal would lead to the collapse of the largest cluster [41]. The red sites form a fractal set of fractal dimension $d_{\mathrm{RS}} = 0.92 \pm 0.07$ (see Fig. 3), which is compatible with the inverse of the correlation length exponent ν that we obtained from the finite-size scaling analysis in Fig. 2, $d_{\mathrm{RS}} = 1/\nu$, as predicted by Coniglio for classical percolation [42]. However the value of $d_{\mathrm{RS}} = 1/\nu$ for the drilling transition is very different from the classical 3D percolation result $1/\nu = 1.1437 \pm 0.0006$ [39]. Figure 3 also shows that the shortest path connecting the top and bottom sides of the largest cluster is a fractal of fractal dimension $d_{\mathrm{SP}} = 1.30 \pm 0.05$. Finally, the backbone of the largest cluster between its bottom and top ends is defined as the set of sites that would carry current if a potential difference is applied

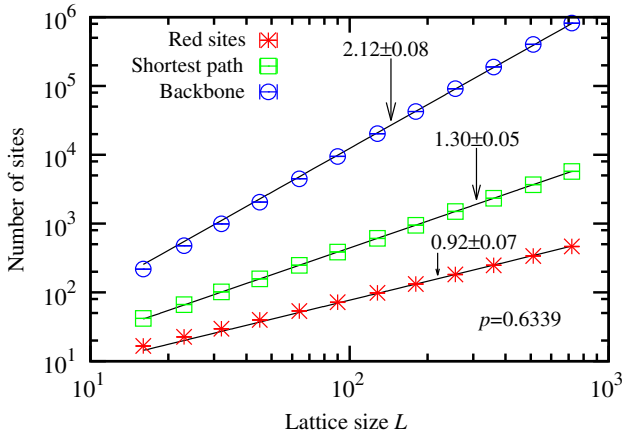

FIG. 3. Number of sites in the backbone of the spanning cluster, length of its shortest path (chemical distance), and red sites in the backbone, measured at $p = p_c = 0.6339$, as a function of the lattice size L. Considering the local slopes of the data, we obtain the following fractal dimensions: $d_{\mathrm{BB}} = 2.12 \pm 0.08$, $d_{\mathrm{SP}} = 1.30 \pm 0.05$, and $d_{\mathrm{RS}} = 0.92 \pm 0.07$. The fractal dimension of the red sites is, within error bars, compatible with the value $1/\nu \approx 0.915$, found from the finite size scaling behavior of the p_c estimators (see Fig. S1), and the relation $d_{\mathrm{RS}} = 1/\nu$ [42]. Here, d_{BB} is larger than in classical three-dimensional percolation, where $d_{\mathrm{BB}} = 1.875 \pm 0.003$ [40,43,44], while d_{SP} is smaller than the classical value $d_{\mathrm{SP}} = 1.3756 \pm 0.0006$ [47]. The solid lines are guides to the eye. To extract the fractal dimensions, we analyzed the local slopes as proposed in Ref. [48]. Results are averages over at least 5×10^3 samples.

between the cluster ends (also known as bi-connected component). The backbone fractal dimension is determined as $d_{\mathrm{BB}} = 2.12 \pm 0.08$, which is larger than in classical 3D percolation, where $d_{\mathrm{BB}} = 1.875 \pm 0.003$ [40,43,44]. Qualitatively, an increase in the backbone fractal dimension is compatible with a simultaneous decrease in the shortest path fractal dimension, since both correspond to a more compact backbone, similar to what is observed in long-range correlated percolation [45,46]. Thus, although the fractal dimension of the largest cluster is similar in both classical percolation and drilling, the internal structure of the largest cluster is significantly different. This implies that transport and mechanical properties of the largest cluster follow a different scaling.

Cluster shape.—Given the highly directional nature of the drilling process, we analyze the symmetry of the different clusters. In particular, we consider them as rigid bodies, consisting of occupied sites at fixed relative positions, and look at the eigenvalues and eigenvectors of their inertia tensors [49,50]. The numerical results show that, when compared to classical percolation clusters, the drilling transition clusters are more anisotropic, their orientations being mainly aligned along the direction of the cube edges (see Supplemental Material for quantitative details [7]).

We now give a rigorous argument for the existence of asymmetric clusters in drilling percolation. Fix some $p \in (p_{2D}, p_c)$, where $p_{2D} \approx 0.5927 < p_c$ is the critical threshold for $2D$ site percolation. Consider a lattice size $L_X \times L_Y \times L_Z$ with $L_X = L_Y = L$ and $L_Z = e^L$, and take a square domain A in its base with side length $k = \sqrt{c_0 \log(L)}$, where c_0 is a positive constant that is smaller than $-\{\log[p(1-p)]\}^{-1}$. Say that the event $\mathcal{S}(A)$ occurred if, along the z direction, no point inside A is drilled but all points on its boundary are. For large L, this event happens with probability at least $L^{c_0 \log[p(1-p)]}$. Consider also two rectangles R_x and R_y in the (x,z) and (y,z) planes, respectively, aligned with A. These rectangles have base length k and height $\exp\{c_1 k\}$, where c_1 is an arbitrary positive constant smaller than the correlation length for two-dimensional percolation with parameter p. The event $\mathcal{R}_x$ (respectively, $\mathcal{R}_y$) indicates the existence of a path crossing R_x (respectively, R_y) from bottom to top that has not been drilled in the y (respectively, x) direction. By our choice of c_1, $\mathcal{R}_x$ and $\mathcal{R}_y$ have a positive probability (uniformly over k); i.e., there exists a $\delta > 0$ such that $P(\mathcal{R}_x) \geq \delta$. In addition, if $\mathcal{S}(A)$ occurs, then there exists a cluster spanning $A \times [0, e^{c_1 k}]$ from bottom to top and whose projection into the (x,y) plane does not extend beyond A. Thus, the probability of finding a cluster of radius k and height $e^{c_1 k}$ is bounded from below by the probability that there exists a square A along the diagonal $x = y$ for which $\mathcal{S}(A) \cap \mathcal{R}_X \cap \mathcal{R}_Y$ occurs, which is greater than

$$1 - \{1 - \delta^2 L^{c_0 \log[p(1-p)]}\}^{L(c_0 \log L)^{-1/2}} \geq 1 - \exp[-c_0^{-1/2} \delta^2 L^{1 + c_0 \log[p(1-p)]} \log(L)^{-1/2}],$$

which converges to unity as L increases. This shows that one expects to have clusters extremely aligned along the z axis, as numerically observed (see for example Fig. S15 of the Supplemental Material [7]). In fact, the same argument can be straightforwardly extended to explain the alignment along the x and y directions, as also observed.

Spanning probability.—To understand the properties of the drilling transition in terms of global connectivity, we consider the spanning probability $\Pi(p)$, defined as the probability to have at least one cluster including sites from the top and bottom of the lattice, at a given value of the control parameter p. Figure 4 shows the spanning probability below the threshold $\Pi(p = 0.63)$, for different lattice aspect ratios. The lattice size is $L_X \times L_Y \times L_Z$ with $L_X = L_Y$ and $L_Z = rL_X$, and the spanning probability is measured in the z direction. At the drilling transition, $p = p_c$, the spanning probability approaches a constant for large lattice sizes (see Supplemental Material, Fig. S9 [7]), similar to what is observed for classical percolation [51,52]. By contrast, for values of p between p_{2D} and p_c, the numerical results suggest a power-law decay of the spanning probability with L_Z, where the exponent increases with the aspect ratio r. For fixed L_X, it decays exponentially with r (see inset of Fig. 4).

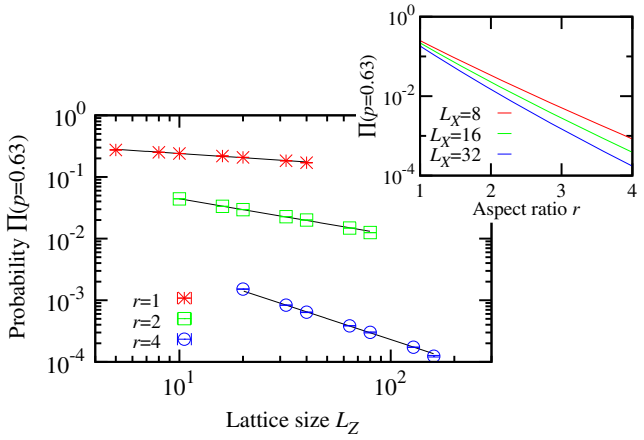

FIG. 4. Main plot: Spanning probability Π, at $p = 0.63 < p_c$, as a function of the lattice size L_Z, for different aspect ratios r. Solid black lines are guides to the eye with slopes, -0.26, -0.58, and -1.22, for $r = 1$, 2, and 4. The inset shows the same probability as a function of the aspect ratio r, for different fixed lattice sizes L_X. Results are based on at least 10^7 samples.

It is possible to establish rigorously the off-critical power-law decay of $\Pi(p)$, modifying the argument for the existence of anisotropic clusters presented above. Specifically, we can show that $\Pi(p) \geq L_X^{-\theta}$, where $\theta = \theta(p, r) > 0$, for any fixed $r > 0$ and $p \in (p_{2D}, p_c)$. For that, let B be the diagonal band $\{(x, y); |x - L_X/2| \leq \alpha n \log(L_X/n), |x - y| < 2n\}$ in the center of the (x, y) face of the cube, where α and n are constants setting the length and width, respectively. Let us say that the event $\mathcal{B}$ occurred if B is free of holes in the (x, y) plane, *i.e.*, if no sites in B are drilled in the z direction. Also say that the event $\mathcal{C}$ occurred if there exists a path σ starting at height $z = 0$ and finishing at height $z = L_Z$ whose projection into the (x, y) plane is contained in B and whose projection into the (x, z) plane [(y, z) plane] consists of sites that have not been drilled in the y direction (x direction). As discussed in detail in the Supplemental Material [7], for well chosen values of α and n, the probability of the event $\mathcal{C}$ is bounded from below by a constant not depending on L_X. Furthermore, $\mathcal{B}$ and $\mathcal{C}$ are independent events. Since their joint occurrence implies the existence of a cluster including sites from the bottom and the top of the lattice, we conclude that

$$\Pi(p) \geq P[\mathcal{B} \cap \mathcal{C}] = P[\mathcal{B}]P[\mathcal{C}]$$
$$\geq \exp\{-c_2 \alpha n \log(L_X)\} c_3 \geq {L_X}^{-\theta},$$

where c_2, c_3, and θ are positive constants that depend on p.

The above argument also shows the existence of anisotropic clusters, sharpening the numerical results presented before. For $p < p_{2D}$, one has $\Pi(p) \sim e^{-c_4 L_X}$, similarly to what happens for uncorrelated random percolation, where c_4 also depends on p. This is due to the fact that the projection of a path spanning the lattice into at least one of the coordinate planes is a path that spans the corresponding face, which has an exponentially small probability in L_X, due to the classical exponential decay of connectivity in the subcritical phase [53,54].

Conclusion.—We find unexpected critical behavior when sequentially drilling holes through a solid cube until it is completely fragmented. At the critical density of drilled holes, a continuous transition is observed in a different universality class than the one of random percolation. We also numerically observe off-critical scale-free behavior that we can justify for a wide range of densities of holes using rigorous arguments. This model is a representative of more complex percolation models where sites are removed in a strongly correlated manner [55–57]. Examples are models where the set of removed sites is given by randomized trajectories, such as the so-called Pacman and interlacement percolation models proposed to study the relaxation at the glass transition [58], enzyme gel degradation [59], and corrosion [60,61], as well as percolation models for distributed computation [62,63]. Other examples are percolation models that explicitly introduce strong directional correlations as in the removal of cylinders [64] and different variants of the four-vertex model [65]. It would be interesting to explore up to which degree these models are in the same universality class or share common features.

While the fractal dimension of the largest fragment is consistent with the one of random percolation, all the other critical exponents are different. This has practical implications as the connectivity and transport properties do change considerably close to the threshold of connectivity. For example, we find the exponent of the order parameter to be substantially larger than for usual percolation, which implies that the drilling transition is less abrupt. Since sites are removed along a line, it is necessary to remove more sites to produce the same effect in the largest fragment. We also find that, compared to usual percolation, the fractal dimension of the backbone is larger, and the one of the shortest path is smaller, corresponding to a more compact backbone and therefore enhanced conductivity properties.

We acknowledge financial support from the ETH Risk Center, the Brazilian institute INCT-SC, and Grant No. FP7-319968 of the European Research Council. K. J. S. acknowledges support by the Swiss National Science Foundation under Grants No. P2EZP2-152188 and No. P300P2-161078. M. R. H. was supported by CNPq Grant No. 248718/2013-4 and by ERC AG "COMPASP". N. A. acknowledges financial support from the Portuguese Foundation for Science and Technology (FCT) under Contracts No. EXCL/FIS-NAN/0083/2012, No. UID/FIS/00618/2013, and No. IF/00255/2013. A. T. is grateful for the financial support from CNPq, Grants No. 306348/2012-8 and No. 478577/2012-5.

*kjs73@cam.ac.uk
†mhilario@mat.ufmg.br
‡vladas@impa.br
§nmaraujo@fc.ul.pt
‖hans@ifb.baug.ethz.ch
¶marcel.thielmann@uni-bayreuth.de
**augusto@impa.br

[1] P. Simon and J. Ihlemann, Appl. Phys. A **63**, 505 (1996).
[2] S. Nolte, C. Momma, H. Jacobs, A. Tünnermann, B. N. Chichkov, B. Wellegehausen, and H. Welling, J. Opt. Soc. Am. B **14**, 2716 (1997).
[3] Y. Kantor, Phys. Rev. B **33**, 3522 (1986).
[4] D. Stauffer, Phys. Rep. **54**, 1 (1979).
[5] D. Stauffer and A. Aharony, *Introduction to Percolation Theory*, 2nd ed. (Taylor and Francis, London, 1994).
[6] G. R. Grimmett, *Percolation, Grundlehren der mathematischen Wissenschaften* Vol. 321 (Springer, Berlin, 1999).
[7] See Supplemental Material at http://link.aps.org/supplemental/10.1103/PhysRevLett.116.055701, which includes Refs. [8–34] for additional information regarding the model, algorithm, and statistics.
[8] R. M. Ziff, Phys. Rev. E **82**, 051105 (2010).
[9] J. Nagler, A. Levina, and M. Timme, Nat. Phys. **7**, 265 (2011).
[10] O. Scholder, Int. J. Mod. Phys. C **20**, 267 (2009).
[11] K. J. Schrenk, N. A. M. Araújo, J. S. Andrade Jr., and H. J. Herrmann, Sci. Rep. **2**, 348 (2012).
[12] H. J. Herrmann and H. E. Stanley, Phys. Rev. Lett. **53**, 1121 (1984).
[13] M. Hilário, V. Sidoravicius, and A. Teixeira, arXiv:1202.1684.
[14] M. E. J. Newman and R. M. Ziff, Phys. Rev. Lett. **85**, 4104 (2000).
[15] M. E. J. Newman and R. M. Ziff, Phys. Rev. E **64**, 016706 (2001).
[16] C. D. Lorenz and R. M. Ziff, Phys. Rev. E **57**, 230 (1998).
[17] N. Jan and D. Stauffer, Int. J. Mod. Phys. C **09**, 341 (1998).
[18] H. G. Ballesteros, L. A. Fernández, V. Martín-Mayor, A. Muñoz Sudupe, G. Parisi, and J. J. Ruiz-Lorenzo, J. Phys. A **32**, 1 (1999).
[19] R. M. Ziff, S. R. Finch, and V. S. Adamchik, Phys. Rev. Lett. **79**, 3447 (1997).
[20] H. N. V. Temperley and E. H. Lieb, Proc. R. Soc. A **322**, 251 (1971).
[21] R. J. Baxter, H. N. V. Temperley, and S. E. Ashley, Proc. R. Soc. A **358**, 535 (1978).
[22] K. J. Schrenk, N. A. M. Araújo, and H. J. Herrmann, Phys. Rev. E **87**, 032123 (2013).
[23] C. D. Lorenz and R. M. Ziff, J. Phys. A **31**, 8147 (1998).
[24] S. Smirnov, in *Proceedings of the International Congress of Mathematicians, Madrid, Spain, 2006*, edited by M. Sanz-Solé, J. Soria, J. L. Varona, and J. Verdera (European Mathematical Society, Zürich, 2006), p. 1421.
[25] M. Matsumoto and T. Nishimura, ACM Trans. Model. Comput. Simul. **8**, 3 (1998).
[26] R. M. Ziff, Comput. Phys. **12**, 385 (1998).
[27] Boost C++ Libraries, http://www.boost.org/.
[28] P. L. Leath, Phys. Rev. B **14**, 5046 (1976).
[29] Z. Alexandrowicz, Phys. Lett. A **80**, 284 (1980).
[30] A. Margolina, H. J. Herrmann, and D. Stauffer, Phys. Lett. A **93**, 73 (1982).
[31] C. Borgs, J. T. Chayes, H. Kesten, and J. Spencer, Commun. Math. Phys. **224**, 153 (2001).
[32] H. Kesten, Commun. Math. Phys. **109**, 109 (1987).
[33] L. D. Landau and E. M. Lifschitz, *Mechanik, Lehrbuch der Theoretischen Physik* Vol. 1 (Harri Deutsch, Frankfurt, 1997), 14th ed..
[34] Intel Math Kernel Library, http://software.intel.com/en-us/intel-mkl.
[35] R. M. Ziff, Phys. Procedia **15**, 106 (2011).
[36] J. L. Jacobsen, J. Phys. A **47**, 135001 (2014).
[37] J. Wang, Z. Zhou, W. Zhang, T. M. Garoni, and Y. Deng, Phys. Rev. E **87**, 052107 (2013).
[38] S. Smirnov and W. Werner, Math. Res. Lett. **8**, 729 (2001).
[39] Y. Deng and H. W. J. Blöte, Phys. Rev. E **72**, 016126 (2005).
[40] H. J. Herrmann, D. C. Hong, and H. E. Stanley, J. Phys. A **17**, L261 (1984).
[41] Numerically, we consider those sites that if removed will disconnect all possible paths between a unit site in the top and one in the bottom faces of the cube. The sites are selected such that their Euclidean distance is maximized.
[42] A. Coniglio, Phys. Rev. Lett. **62**, 3054 (1989).
[43] M. D. Rintoul and H. Nakanishi, J. Phys. A **27**, 5445 (1994).
[44] Y. Deng and H. W. J. Blöte, Phys. Rev. E **70**, 046106 (2004).
[45] S. Prakash, S. Havlin, M. Schwartz, and H. E. Stanley, Phys. Rev. A **46**, R1724 (1992).
[46] K. J. Schrenk, N. Posé, J. J. Kranz, L. V. M. van Kessenich, N. A. M. Araújo, and H. J. Herrmann, Phys. Rev. E **88**, 052102 (2013).
[47] Z. Zhou, J. Yang, Y. Deng, and R. M. Ziff, Phys. Rev. E **86**, 061101 (2012).
[48] P. Grassberger, Physica (Amsterdam) **262A**, 251 (1999).
[49] J. Rudnick and G. Gaspari, Science **237**, 384 (1987).
[50] M. L. Mansfield and J. F. Douglas, J. Chem. Phys. **139**, 044901 (2013).
[51] J. L. Cardy, J. Phys. A **25**, L201 (1992).
[52] S. Smirnov, C. R. Acad. Sci. Paris, Ser. I **333**, 239 (2001).
[53] M. V. Menshikov, Dokl. Akad. Nauk SSSR **288**, 1308 (1986); [Sov. Phys. Dokl. vol, page year].
[54] M. Aizenman and D. J. Barsky, Commun. Math. Phys. **108**, 489 (1987).
[55] N. A. M. Araújo, P. Grassberger, B. Kahng, K. J. Schrenk, and R. M. Ziff, Eur. Phys. J. Spec. Top. **223**, 2307 (2014).
[56] M. Hilário and V. Sidoravicius, arXiv:1509.06204.
[57] X.-W. Liu, Y. Deng, and J. L. Jacobsen, Phys. Rev. E **92**, 010103(R) (2015).
[58] R. Pastore, M. P. Ciamarra, and A. Coniglio, Fractals **21**, 1350021 (2013).
[59] T. Abete, A. de Candia, D. Lairez, and A. Coniglio, Phys. Rev. Lett. **93**, 228301 (2004).
[60] A.-S. Sznitman, Ann. Probab. **37**, 1715 (2009).
[61] A.-S. Sznitman, Ann. Math. **171**, 2039 (2010).
[62] D. Coppersmith, P. Tetali, and P. Winkler, SIAM J. Discrete Math. **6**, 363 (1993).
[63] P. Winkler, Random Struct. Algorithms **16**, 58 (2000).
[64] J. Tykesson and D. Windisch, Probab. Theory Relat. Fields **154**, 165 (2012).
[65] G. Pete, Ann. Probab. **36**, 1711 (2008).